JACC: CARDIOVASCULAR INTERVENTIONS VOL. 11, NO. 14, 2018

PUBLISHED BY ELSEVIER

Neoatherosclerosis in Patients With Coronary Stent Thrombosis

Findings From Optical Coherence Tomography Imaging (A Report of the PRESTIGE Consortium)

Michael Joner, MD,[a,k] Tobias Koppara, MD,[b,k] Robert A. Byrne, MB, BCh, PhD,[a,k] Maria Isabel Castellanos, PhD,[a,k] Jonas Lewerich, MS,[a] Julia Novotny, MD,[c] Giulio Guagliumi, MD,[d] Erion Xhepa, MD,[a] Tom Adriaenssens, MD,[e] Thea C. Godschalk, MSc,[f] Nikesh Malik, MD, PhD,[g] Fernando Alfonso, MD,[h] Tomohisa Tada, MD,[a] Franz-Josef Neumann, MD,[i] Walter Desmet, MD, PhD,[e] Jurrien M. ten Berg, MD, PhD,[e] Anthony H. Gershlick, MD,[g] Laurent J. Feldman, MD, PhD,[j] Steffen Massberg, MD,[c,k] Adnan Kastrati, MD,[a,k] on behalf of the Prevention of PRESTIGE Investigators

ABSTRACT

OBJECTIVES The purpose of this study was to assess neoatherosclerosis in a registry of prospectively enrolled patients presenting with stent thrombosis using optical coherence tomography.

BACKGROUND In-stent neoatherosclerosis was recently identified as a novel disease manifestation of atherosclerosis after coronary stent implantation.

METHODS Angiography and intravascular optical coherence tomography were used to investigate etiologic factors of neoatherosclerosis in patients presenting with stent thrombosis >1 year after implantation (very late stent thrombosis [VLST]). Clinical data were collected according to a standardized protocol. Optical coherence tomographic acquisitions were analyzed in a core laboratory. Cox regression analysis was performed to identify factors associated with the formation of neoatherosclerosis and plaque rupture as a function of time.

RESULTS Optical coherence tomography was performed in 134 patients presenting with VLST. A total of 58 lesions in 58 patients with neoatherosclerosis were compared with 76 lesions in 76 patients without neoatherosclerosis. Baseline characteristics were similar between groups. In-stent plaque rupture was the most frequent cause (31%) in all patients presenting with VLST. In patients with neoatherosclerosis, in-stent plaque rupture was identified as the cause of VLST in 40 cases (69%), whereas uncovered stent struts (n = 22 [29%]) was the most frequent cause in patients without neoatherosclerosis. Macrophage infiltration was significantly more frequent in optical coherence tomographic frames with plaque rupture compared with those without (50.2% vs. 22.2%; $p < 0.0001$), whereas calcification was more often observed in frames without plaque rupture (17.2% vs. 4%; $p < 0.0001$). Implantation of a drug-eluting stent was significantly associated with the formation of neoatherosclerosis ($p = 0.02$), whereas previous myocardial infarction on index percutaneous coronary intervention was identified as a significant risk factor for plaque rupture in patients with neoatherosclerosis ($p = 0.003$). No significant difference was observed in thrombus composition between patients with or without neoatherosclerosis.

CONCLUSIONS Neoatherosclerosis was frequently observed in patients with VLST. Implantation of a drug-eluting stent was significantly associated with neoatherosclerosis formation. In-stent plaque rupture was the prevailing pathological mechanism and often occurred in patients with neoatherosclerosis and previous myocardial infarction at index percutaneous coronary intervention. Increased macrophage infiltration heralded plaque vulnerability in our study and might serve as an important indicator. (J Am Coll Cardiol Intv 2018;11:1340–50) © 2018 by the American College of Cardiology Foundation.

From [a]Deutsches Herzzentrum München, Technische Universität München, Munich, Germany; [b]Klinik und Poliklinik für Innere Medizin I, Klinikum Rechts der Isar, Technische Universität München, Munich, Germany; [c]Medizinische Klinik und Poliklinik I, Ludwig-Maximilians-Universität, Munich, Germany; [d]Azienda Ospedaliera Papa Giovanni XXIII, Bergamo, Italy; [e]Department of Cardiology, University Hospitals Leuven, and Department of Cardiovascular Sciences, KU Leuven, Leuven, Belgium; [f]Department of Cardiology, St. Antonius Hospital, Nieuwegein, the Netherlands; [g]Department of Cardiovascular Sciences,

ISSN 1936-8798/$36.00 https://doi.org/10.1016/j.jcin.2018.02.029

In-stent neoatherosclerosis was recently identified as a novel disease manifestation of atherosclerosis in coronary arteries within the forming neointima following stent implantation (1). Although its exact prevalence in clinical practice remains unknown to date, autopsy studies have reported a frequency of 31% in 157 cases with drug-eluting stents (DES) and 16% in 142 cases with bare metal stents (BMS), despite a longer duration of implantation in the latter (1). The prevalence and characteristics of neoatherosclerosis in living patients have been investigated using data acquired from intravascular imaging modalities such as intravascular ultrasound, near-infrared spectroscopy, and optical coherence tomography (OCT) by optical frequency domain imaging. Lipid-laden neointimal tissue was reported to be a frequent finding in patients presenting late (≥5 years) after stent implantation and most often manifested in the clinical setting of in-stent restenosis (2). Recently, Taniwaki et al. (3) reported intravascular imaging findings in 64 patients with first- and second-generation DES presenting with very late stent thrombosis (VLST) and found neoatherosclerosis to be the underlying mechanism in 27.6% of cases. Despite the obvious contribution of neoatherosclerosis to the development of VLST, precise understanding of causative associations and interaction with other contributing factors is lacking to date. We therefore aimed to investigate the role of neoatherosclerosis in a large prospective database of patients with stent thrombosis presenting to 29 participating clinical centers with intravascular imaging capability throughout Europe (PRESTIGE [Prevention of Late Stent Thrombosis by an Interdisciplinary Global European Effort]) and provide insights into the timing and frequency of neoatherosclerosis in a broad patient population with first-generation and newer generation DES as well as BMS. One of the main aims of this study was to find meaningful predictors of neoatherosclerosis formation in patients presenting with VLST.

SEE PAGE 1351

METHODS

STUDY POPULATION AND PATIENT TREATMENT. Consecutive patients presenting with definite stent thrombosis undergoing percutaneous coronary intervention at 29 participating centers with OCT imaging capability were prospectively enrolled in the multicenter PRESTIGE registry using a centralized telephone registration system. A list of participating centers has been previously reported (4). Definite stent thrombosis was defined according to Academic Research Consortium criteria (5). Clinical, procedural, and imaging data were collected according to a standardized protocol and entered by site investigators in a central electronic database (Open Clinica, Leuven Coordinating Centre, Leuven, Belgium) checked by centralized monitoring queries. Classification of underlying stent type was previously reported (6,7). The study complied with the Declaration of Helsinki. The ethical review committee at each participating institution approved the study, and all patients provided written informed consent.

SUBGROUP SELECTION AND DEFINITION OF NEOATHEROSCLEROSIS. For the present analysis, only patients presenting with VLST (≥12 months) were selected and split into 2 main strata, defined by the presence or absence of neoatherosclerosis (stratum 1), whereas patients with neoatherosclerosis were further divided into subgroups with or without identified plaque rupture within the target vascular segment resulting in VLST as identified by the optical coherence tomography core laboratory (stratum 2) (**Figure 1**). Neoatherosclerosis was defined as the presence of a fibroatheroma or fibrocalcific plaque within the neointima of a stented arterial segment. Fibroatheroma was characterized by a signal-poor region displaying high attenuation with diffuse borders and a lateral extension of at least 1 quadrant, as previously defined (3). Fibrocalcific plaque was defined as signal-poor region with low attenuation and clearly visible demarcation of its borders extending over ≥1 quadrant in its circumference. Macrophage infiltration was defined as a signal-rich

ABBREVIATIONS AND ACRONYMS

BMS = bare-metal stent(s)

DES = drug-eluting stent(s)

OCT = optical coherence tomography

ST = stent thrombosis

VLST = very late stent thrombosis

University of Leicester & Leicester NIHR Cardiovascular Biomedical Research Unit, Glenfield Hospital, Leicester, United Kingdom; [h]Hospital Universitario de La Princesa, Madrid, Spain; [i]Universitäts-Herzzentrum Freiburg-Bad Krozingen, Bad Krozingen, Germany; [j]Département de Cardiologie, AP-HP, DHU FIRE, U-1148 INSERM, Hôpital Bichat, Paris, France; and the [k]German Centre for Cardiovascular Research, partner site Munich Heart Alliance, Munich, Germany. The research leading to these results has received funding from the European Union Seventh Framework Programme (FP7/2007-2013) under grant agreement HEALTH-F2-2010-260309 (PRESTIGE). Funding for open-access publication is provided by the European Commission. The authors have reported that they have no relationships relevant to the contents of this paper to disclose.

Manuscript received January 7, 2018; revised manuscript received February 15, 2018, accepted February 17, 2018.

FIGURE 1 Study Flowchart

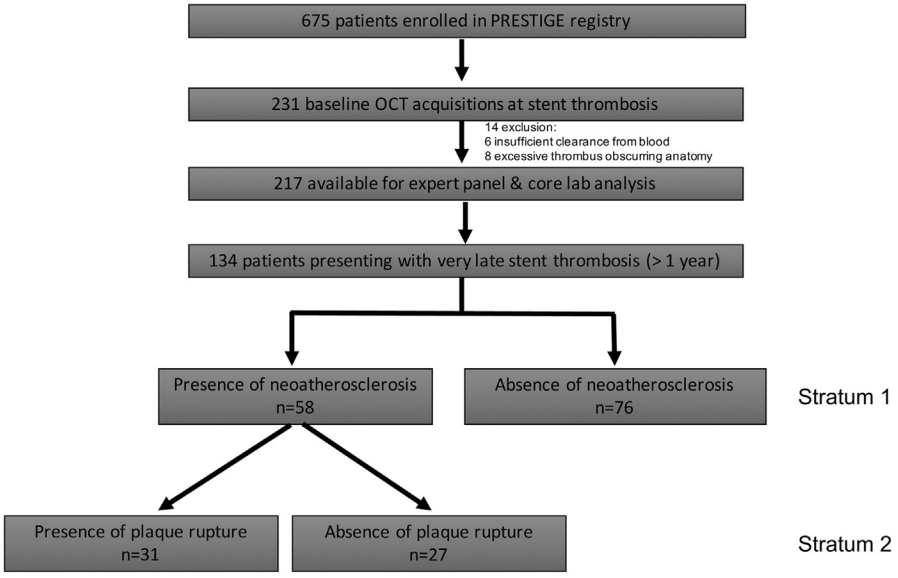

Study flow of patients according to the presence or absence of neoatherosclerosis (stratum 1) and plaque rupture (stratum 2). OCT = optical coherence tomography; PRESTIGE = Prevention of Late Stent Thrombosis by an Interdisciplinary Global European Effort.

band with significant light attenuation within the endoluminal neointimal tissue or low-signal intensity area followed by a signal-rich band with significant attenuation within the endoluminal neointimal tissue.

OCT QUANTITATIVE ANALYSIS. Raw data from OCT acquisitions were collected and sent to a centralized core laboratory (ISAResearch Center, Munich, Germany) for off-line analyses. Each OCT sequence was assessed and measured by independent readers experienced in OCT analysis, blinded to patient characteristics and the timing of stent thrombosis, as previously described (7). Reasons for exclusion of OCT pull-back evaluation were insufficient image quality due to poor clearance of blood, missed region of interest with incomplete stent visualization, excessive remaining thrombus obscuring stent assessment, or presence of imaging artifacts precluding analysis. Nonanalyzable frames were defined as frames with less than a total of 45° of visible luminal border (e.g., because of the presence of thrombus or a side branch). Stent struts located across the ostium of side branches were excluded from analysis of coverage and apposition. Quantitative and morphometric analyses were performed every 1 mm along the entire target segment. Dedicated software (St. Jude Medical, St. Paul, Minnesota) was used for quantification. Further details and definitions have been previously reported (7).

To evaluate the distribution of underlying plaque type in cases with neoatherosclerosis and in-stent plaque rupture, analysis of lesion morphology was performed every other frame. The presence or absence of fibroatheroma and signal attenuation indicative of macrophages (at least 1 quadrant of significant signal attenuation) was recorded on a nominal scale, while the presence of any calcification and neoangiogenesis was also documented. Minimum fibrous cap thickness was derived by measuring the distance of the hyperreflective fibrous cap signal band toward the endoluminal surface in a minimum of 3 locations per frame, avoiding regions where thrombus obscured underlying lesion morphology. Thin-cap fibroatheroma was defined as fibroatheroma exhibiting a minimum cap thickness of ≤85 μm thickness.

OCT QUALITATIVE ANALYSIS. An imaging adjudication committee adjudicated the findings at the time of stent thrombosis on the basis of systematic review of all acquired OCT pull-backs according to a prespecified protocol as previously reported (7). If no single dominant finding was assessed, this was recorded. Additional findings that were not considered dominant were adjudicated as contributory bystanders. The decision was made by consensus. The

categories under consideration for visual adjudication have been previously reported (7).

HISTOPATHOLOGIC SAMPLING AND ANALYSIS OF THROMBUS ASPIRATIONS. Patients presenting with stent thrombosis undergoing successful catheter thrombectomy at participating centers were eligible for inclusion in this substudy as previously described (4). After crossing the lesion with a standard guidewire, a thrombectomy catheter was advanced to the target lesion, and thrombus aspiration was performed according to standard practice. Thrombus was collected according to a standardized protocol. Immediately after thrombus harvest, specimens were fixed in formalin 4% and shipped to the core laboratory for thrombus analysis (Deutsches Herzzentrum München, Munich, Germany). At the core laboratory, thrombus specimens were embedded in paraffin after 48 hours of formalin fixation. Serial cross-sections of all thrombi were then cut with 5-μm thickness. Paraffin-embedded tissue sections were deparaffinized by immersion in xylene and rehydrated in decreasing concentrations of ethanol. Sections were stained with hematoxylin and eosin and Luna stain. For immunohistochemistry, antigen retrieval was performed as previously described (4). Neutrophil extracellular traps were identified by their expression of neutrophil elastase using a rabbit polyclonal neutrophil elastase antibody (Ab68672, Abcam, Cambridge, United Kingdom). Rabbit immunoglobulin G was used as a control. Goat antirabbit Alexa Fluor 594 (Invitrogen, Carlsbad, California) was used as a secondary antibody. Deoxyribonucleic acid was stained with Hoechst 33342 Solution (Invitrogen). Cells and neutrophil extracellular traps were quantified in 4 visual fields using a 40× objective (176 × 131 μm). The results were extrapolated to cells per square millimeter. Preconditions to quantify neutrophil extracellular trap formation and data acquisition were in agreement with previously published methods (4).

STATISTICAL ANALYSIS. Continuous data are presented as mean ± SD or median (interquartile range [IQR]). Categorical data are presented as observed frequencies and proportions. Patients were analyzed according to the presence or absence of neoatherosclerosis (stratum 1). In a second analysis, the subgroup of patients with any type of neoatherosclerosis was further categorized by the presence or absence of plaque rupture within the target vascular segment resulting in VLST (stratum 2). Differences between groups were assessed for statistical significance using the Wilcoxon rank sum test or a Kruskal-Wallis test for continuous data and the chi-square test (or Fisher exact test when the expected cell value was <5) for categorical variables. All tests were 2 sided and assessed at a significance level of 5%. Because of the exploratory nature of the analysis, no adjustment was made for multiple testing. Agreement statistics using kappa coefficients and asymptotic tests to derive probability distributions were calculated to test interobserver and intraobserver variability for nominal (qualitative) variables assessed during optical coherence tomography core laboratory analysis. Multivariate Cox proportional hazards regression analysis was applied to identify factors associated with the formation of neoatherosclerosis and to further examine factors associated with plaque rupture in the subgroup of patients with neoatherosclerosis. Hazard ratios with their 95% confidence intervals were computed. To avoid overfitting of the regression model, selection of covariates in the multivariate Cox regression model was performed using the least absolute shrinkage and selection operator regression method after entering all baseline and procedural characteristics as candidates (R package glmnet, version 2.0-13). The resulting variables for the multivariate Cox regression model assessing associations with neoatherosclerosis

TABLE 1 Clinical Characteristics of Patients With and Those Without Neoatherosclerosis at the Time Point of Presentation With Very Late Stent Thrombosis

	Patients With Neoatherosclerosis (n = 58)	Patients Without Neoatherosclerosis (n = 76)	p Value
Age (yrs)	60.7 ± 11.5	62.7 ± 12.1	0.33
Body mass index (kg/m^2)	27.1 ± 4.1	27.0 ± 4.3	0.91
Male	50/58 (86.2)	66/76 (86.8)	0.92
Diabetes	9/58 (15.5)	14/76 (18.4)	0.66
Insulin dependent	1/58 (1.7)	2/74 (2.7)	0.71
Hypercholesterolemia	50/53 (94.3)	61/65 (93.8)	0.91
Arterial hypertension	19/56 (33.9)	32/72 (44.4)	0.23
Active smoker	20/57 (35.1)	22/73 (30.1)	0.55
Severely impaired left ventricular function*	1/58 (1.7)	3/76 (4)	0.45
Prior bypass operation	2/58 (3.4)	4/76 (5.3)	0.62
Prior myocardial infarction	29/58 (50)	41/76 (53.9)	0.65
Renal insufficiency	2/58 (3.5)	4/76 (5.3)	0.62
Clinical presentation			0.10
ST-segment elevation myocardial infarction	44/57 (77.2)	57/74 (77.0)	
Non-ST-segment elevation myocardial infarction	13/57 (22.8)	12/74 (16.2)	
Unstable angina	0/57 (0)	5/74 (6.8)	
Antiplatelet therapy			
Dual antiplatelet therapy	7/58 (12.1)	13/75 (17.3)	0.40
Aspirin	43/58 (74.1)	63/72 (87.5)	0.05
$P2Y_{12}$ inhibitor	12/57 (21.1)	11/73 (15.1)	0.37
Oral anticoagulation	5/52 (9.6)	4/70 (5.7)	0.41

Values are mean ± SD or n/N (%). *Ejection fraction <30%.

TABLE 2 Angiographic and Procedural Characteristics of Patients With and Those Without Neoatherosclerosis

	Patients With Neoatherosclerosis (n = 58)	Patients Without Neoatherosclerosis (n = 76)	p Value
Culprit vessel			0.25
LM	1/55 (1.8)	1/74 (1.3)	
LAD	20/55 (36.4)	32/74 (43.2)	
LCx	8/55 (14.5)	11/74 (14.9)	
RCA	26/55 (47.3)	23/74 (31.1)	
LAD/LCx	0/55 (0)	3/74 (4.1)	
Unknown	0/55 (0)	1/74 (1.3)	
SVG lesion	2/55 (3.8)	2/71 (2.8)	0.77
Bifurcation lesion	9/52 (17.3)	11/71 (15.5)	0.79
Number of stents implanted in vessel with ST	81	113	
Stent type at index procedure			
BMS	39/81 (48.2)	21/113 (19)	<0.0001
DES G1	21/81 (25.9)	49/113 (43.4)	0.13
DES G2	12/81 (15)	37/113 (32.7)	0.0002
Unknown	8/81 (9.9)	6/113 (5.3)	0.6
TIMI flow grade at presentation			0.85
0/1	46/57 (80.7)	55/74 (74.3)	
2	6/57 (10.5)	11/74 (14.9)	
3	4/57 (7)	6/74 (8.1)	
Thrombus aspiration	52/58 (89.7)	68/75 (90.7)	0.85
Balloon angioplasty	53/58 (91.4)	62/73 (84.9)	0.24
Glycoprotein receptor antagonist	19/56 (33.9)	22/67 (32.8)	0.29

Values are n/N (%).

BMS = bare-metal stent(s); DES = drug-eluting stent(s); G1 = first-generation; G2 = second-generation; LAD = left anterior descending coronary artery; LCx = left circumflex coronary artery; RCA = right coronary artery; ST = stent thrombosis; SVG = saphenous vein graft; TIMI = Thrombolysis In Myocardial Infarction.

formation were age and stent type; the resulting variables for the multivariate Cox regression model assessing associations with plaque rupture in patients with neoatherosclerosis were stent type, diabetes, smoking status, previous myocardial infarction, bifurcation stenting, and TIMI (Thrombolysis In Myocardial Infarction) flow grade before intervention. Missing baseline data were imputed by using the predictive mean matching function (R package mice, version 2.46). The statistical analysis was performed using JMP Pro version 12.0 (SAS Institute, Cary, North Carolina), SPSS version 22 (IBM, Armonk, New York), and R version 3.3.4 (R Foundation for Statistical Computing, Vienna, Austria).

RESULTS

A total of 675 patients with stent thrombosis were enrolled in the PRESTIGE stent thrombosis registry. Of these, 231 underwent OCT imaging at the time of stent thrombosis. Fourteen patients had image quality precluding further analysis (poor quality due to blood contamination [n = 6] or excessive remaining thrombus [n = 8]). Of the remaining 217 patients, those presenting very late (n = 134) constituted the primary study cohort for the present analysis (Figure 1).

Baseline clinical characteristics of patients at the time point of index stenting procedure are listed in Online Table Ia and do not show any significant difference between the groups with and without neoatherosclerosis except for age. Patients with neoatherosclerosis were significantly younger than those without neoatherosclerosis.

No significant differences were observed between the 2 groups regarding the baseline characteristics recorded at the time of VLST (Table 1). The median time from index stenting to presentation with VLST was 5.95 years (IQR: 2.99 to 8.65 years). Lesion and procedural characteristics of patients at the time point of VLST according to the presence or absence of neoatherosclerosis are reported in Table 2. A total of 81 stents were implanted in target vessels of patients presenting with VLST and neoatherosclerosis: 39 BMS (48.2%), 21 first-generation DES (25.9%), 12 newer generation DES (15%), and 8 stents of unknown type (9.9%). A total of 113 stents were implanted in target vessels of patients presenting with VLST not exhibiting neoatherosclerosis: 21 BMS (19%), 49 first-generation DES (43.4%), 37 newer generation DES (32.7%), and 6 stents of unknown type (5.3%). The median duration of implantation from index stenting to VLST was 4.52 years (IQR: 2.1 to 6.5 years) for DES and 8.24 years (IQR: 5.0 to 11.49 years) for BMS ($p < 0.0001$) (Figure 2). Lesion and procedural characteristics of patients at the time point of VLST according to the presence or absence of plaque rupture are reported in Table 3, and lesion characteristics at the time point of index stenting are reported in Online Table Ia. Clinical characteristics in patients with and without plaque rupture are listed in Online Table Ib, whereas angiographic and procedural characteristics according to the presence or absence of plaque rupture are reported in Online Table II.

OPTICAL COHERENCE TOMOGRAPHY CORE LABORATORY ANALYSIS. OCT morphometric data according to the time of presentation are reported in Table 4. Although minimum and mean stent area were significantly larger in patients with neoatherosclerosis, minimum and mean luminal area showed the opposite trend, with significantly smaller minimum luminal area in patients with neoatherosclerosis. A stent expansion index <0.8 was observed in 19.6% of patients with neoatherosclerosis and in 54.2% of patients without neoatherosclerosis ($p = 0.0001$). OCT morphometric data according to time of presentation in patients

FIGURE 2 Distribution of Stents

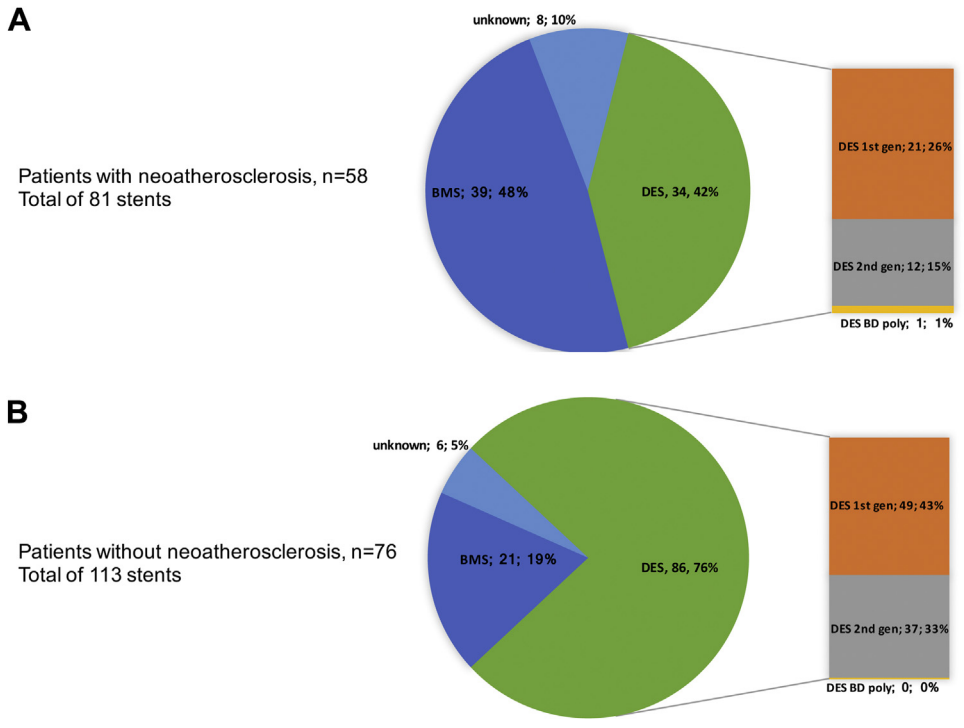

Distribution of bare-metal stents (BMS), first- and second-generation drug-eluting stents (DES), and DES with biodegradable polymer (BD poly) coating in patients with **(A)** and without **(B)** neoatherosclerosis.

with and without plaque rupture are listed in Online Table III.

OCT analysis of stent-vessel interaction for each lesion according to the presence or absence of neoatherosclerosis is reported in **Table 5**. A total of 58 lesions in 58 patients with neoatherosclerosis (mean 25.1 ± 14.6 frames per patient) were quantitatively analyzed and compared with 76 lesions in 76 patients without neoatherosclerosis (mean 25.6 ± 12.1 frames per patient).

The number of lesions with any frame showing uncovered struts was significantly larger in patients without neoatherosclerosis compared with those with neoatherosclerosis. The mean number of frames with uncovered stent struts and the maximum length of consecutive uncovered stent struts were also significantly larger in patients without neoatherosclerosis compared with those with neoatherosclerosis. The same trend was observed for the number and maximum length of consecutive frames covered by thrombus. The number of malapposed stent struts and the maximum length of consecutive malapposed stent struts were also significantly larger in patients without neoatherosclerosis.

Neointimal lesion morphology in patients with neoatherosclerosis was assessed in a total of 6,273 frames with sufficient image quality permitting core laboratory assessment; of those, 3,283 frames were located within the stented segments (52.3%), whereas 2,990 frames were located within the adjacent nonstented segments (47.7%) within 5 mm proximal or distal to the stented segment. Of the 6,273 frames, 186 (3%) were classified as fibroatheroma (19 thin-cap fibroatheroma and 165 thick-cap fibroatheroma) and 301 (4.8%) as plaque rupture; the remaining frames were classified as pathological intimal thickening and fibrocalcific plaque (in the absence of optical coherence tomography–defined necrotic core) (n = 5,787 [92.3%]); a total of 27 frames (0.4%) had significant neovascularization; calcification was seen in 1,120 frames (17.6%). Macrophage infiltration into neointimal tissue was observed in 1,582 frames (25.2%); of the 301 frames with plaque rupture, 12 (4%) showed additional fibroatheroma in adjacent frames,

TABLE 3 Clinical Characteristics of Patients With and Those Without Plaque Rupture at the Time Point of Presentation With Very Late Stent Thrombosis

	Patients With Neoatherosclerosis and Rupture (n = 31)	Patients With Neoatherosclerosis Without Rupture (n = 27)	p Value
Age (yrs)	61.2 ± 11.8	60.2 ± 11.3	0.65
Body mass index (kg/m^2)	28.0 ± 4.0	26.1 ± 4.0	0.23
Male	28/31 (90.3)	22/27 (81.5)	0.33
Diabetes	4/31 (12.9)	5/27 (18.5)	0.56
Insulin dependent	0/31 (0)	1/27 (3.7)	0.28
Hypercholesterolemia	26/28 (92.9)	24/25 (96)	0.62
Arterial hypertension	8/30 (26.7)	11/26 (42.3)	0.22
Active smoker	11/30 (36.7)	9/27 (33.3)	0.79
Severely impaired left ventricular function	1/31 (3.2)	0/27 (0)	0.35
Prior bypass operation	2/31 (6.5)	0/27 (0)	0.18
Prior myocardial infarction	16/31 (51.6)	13/27 (48.2)	0.79
Renal insufficiency	1/31 (3.2)	1/27 (3.7)	0.92
Clinical presentation			0.07
ST-segment elevation myocardial infarction	26/30 (86.7)	18/27 (66.7)	
Non-ST-segment elevation myocardial infarction	4/30 (13.3)	9/27 (33.3)	
Antiplatelet therapy			
Dual antiplatelet therapy	2/31 (6.5)	5/27 (18.5)	0.16
Aspirin	19/31 (61.3)	24/27 (88.9)	0.02
$P2Y_{12}$ inhibitor	5/30 (16.7)	7/27 (25.9)	0.39
Oral anticoagulation	4/28 (14.3)	1/24 (4.2)	0.22

Values are mean ± SD or n/N (%).

TABLE 4 Optical Coherence Tomographic Morphometric Analysis in Patients With and Those Without Neoatherosclerosis

	Patients With Neoatherosclerosis (n = 58)	Patients Without Neoatherosclerosis (n = 76)	p Value
Minimum stent area (mm^2)	6.83 ± 2.30	5.63 ± 2.37	0.001
Mean stent area (mm^2)	8.20 ± 2.30	6.96 ± 2.51	0.001
Minimum stent diameter (mm)	2.86 ± 0.55	2.61 ± 0.51	0.004
Mean stent diameter (mm)	3.19 ± 0.45	2.93 ± 0.50	0.001
Minimum luminal area (mm^2)	2.73 ± 1.62	3.80 ± 2.33	0.002
Mean luminal area (mm^2)	4.87 ± 1.87	5.64 ± 2.72	0.18
Minimum luminal diameter (mm)	1.78 ± 0.53	2.10 ± 0.63	0.002
Mean luminal diameter (mm)	2.40 ± 0.49	2.59 ± 0.58	0.12
Proximal luminal area (mm^2)	8.30 ± 3.21	7.61 ± 3.22	0.20
Proximal luminal diameter (mm)	3.17 ± 0.65	3.04 ± 0.66	0.20
Distal luminal area (mm^2)	5.27 ± 2.40	5.92 ± 2.83	0.28
Distal luminal diameter (mm)	2.52 ± 0.57	2.70 ± 0.61	0.20
Reference area (mm^2)	6.70 ± 2.50	6.80 ± 2.42	0.69
Reference diameter (mm)	2.83 ± 0.54	2.88 ± 0.51	0.58
Expansion index	1.07 ± 0.34	0.86 ± 0.30	0.001
Stent expansion <80%	10/51 (19.6)	32/59 (54.2)	0.0001

Values are mean ± SD or n/N (%).

and 151 (50.2%) showed macrophage infiltration. Calcification was also observed in 12 frames (4%) with plaque rupture. Mean cap thickness measured 115 ± 15 μm. Macrophage infiltration was more often observed in frames with plaque rupture versus those without (151 of 301 [50.2%] vs. 1,431 of 5,972 [24%]; $p < 0.0001$). Conversely, calcification was more frequently observed in frames without plaque rupture (1,108 of 5,972 [18.6%] vs. 12 of 301 [4%]; $p < 0.0001$). The kappa coefficient for detection of macrophage infiltration was 0.81 ($p < 0.001$) for interobserver variability and 0.74 ($p < 0.001$) for intraobserver variability; the kappa coefficient for detection of calcification was 0.85 ($p < 0.001$) for interobserver variability and 0.85 ($p < 0.001$) for intraobserver variability. OCT analysis of stent-vessel interaction according to the time of presentation in patients with and without plaque rupture is reported in Online Table IV.

IMAGING ADJUDICATION COMMITTEE ANALYSIS OF FINDINGS. Representative images of dominant findings for patients presenting with VLST in the absence or presence of neoatherosclerosis are shown in Online Figures Ia and Ib, respectively. Although plaque rupture was found to be the dominant mechanism of VLST (40 of 48 [69%]) in the majority of patients beyond the 1-year time frame, 18 of 58 patients (31%) presented with dominant mechanisms other than plaque rupture (uncovered struts, n = 5; malapposition, n = 2; severe stenosis, n = 4; underexpansion, n = 1; no dominant cause, n = 4; edge segment disease, n = 2). The frequency of neoatherosclerosis among patients with BMS and DES is shown in **Figure 2**.

IDENTIFICATION OF FACTORS ASSOCIATED WITH NEOATHEROSCLEROSIS FORMATION. Multivariate Cox regression analysis showed a 2.2-fold increased risk to develop neoatherosclerosis after implantation of DES relative to BMS (hazard ratio: 2.22; 95% confidence interval: 1.15 to 4.30; $p = 0.02$) (**Figure 3A**). The median follow-up duration was 7.8 years (IQR: 5.0 to 11.5 years) for patients with neoatherosclerosis and 4.5 years (IQR: 2.1 to 6.9 years) for patients without neoatherosclerosis.

IDENTIFICATION OF FACTORS ASSOCIATED WITH PLAQUE RUPTURE. Multivariate Cox regression analysis showed a 4.9-fold higher risk for plaque rupture in patients with neoatherosclerosis and previous myocardial infarction (hazard ratio: 4.87; 95% confidence interval: 1.73 to 13.73; $p = 0.003$) (**Figure 3B**). The median follow-up duration was 8.7 years (IQR: 6.3 to 12.5 years) for patients with plaque rupture and 6.9 years (IQR: 4.8 to 10.3 years) for patients without plaque rupture.

COMPARISON OF THROMBUS ASPIRATION BETWEEN PATIENTS WITH AND WITHOUT NEOATHEROSCLEROSIS. A total of 67 patients presenting with VLST underwent thrombus aspiration and were separated into 37 patients with and 30 without neoatherosclerosis (Online Figure II). Median duration was 2,557 days (IQR: 1,419 to 4,166 days) in patients with neoatherosclerosis and 1,203 days (IQR: 598 to 1,774 days) in patients without neoatherosclerosis (p = 0.01). There were no significant differences in the numbers of leukocytes, neutrophils, eosinophils, and neutrophil extracellular traps among thrombus aspirations taken from patients with and without neoatherosclerosis.

TABLE 5 Optical Coherence Tomographic Analysis of Stent-Vessel Interaction in Patients With and Those Without Neoatherosclerosis

	Patients With Neoatherosclerosis (n = 58)	Patients Without Neoatherosclerosis (n = 76)	p Value
Lesion-level analysis			
Number of frames analyzed per lesion	25.1 ± 14.6	25.6 ± 12.1	0.83
Any frames with thrombus	57/58 (98.3)	69/75 (92)	0.11
Any frames with malapposed struts	14/58 (24.1)	36/75 (48)	0.004
Any frames with uncovered struts	19/58 (32.8)	53/75 (70.7)	<0.001
Any frames with interstrut cavities	11/58 (19)	24/75 (32)	0.09
Any frames with neoatherosclerosis	58/58 (100)	0/765 (0)	<0.001
Frame-level analysis			
Coverage	n = 1,332	n = 1,643	
Frames with uncovered struts (n)	1.2 ± 2.4	4.0 ± 5.4	<0.0001
Frames with uncovered struts (%)	0 (0–8.0)	11.5 (0–32.1)	<0.0001
Maximum length of consecutive uncovered struts (mm)	0.8 ± 1.7	2.9 ± 3.9	<0.0001
Frames with struts covered by thrombus (n)	0.7 ± 1.6	2.8 ± 3.8	<0.0001
Frames with struts covered by thrombus (%)	0 (0–0)	7.3 (0–21.4)	<0.0001
Maximum length of frames containing thrombus (mm)	8.3 ± 8.4	10.1 ± 8.3	0.04
Frames with uncovered struts or struts covered by thrombus (n)	1.9 ± 3.2	6.8 ± 7.8	<0.0001
Frames with uncovered struts or struts covered by thrombus (%)	0 (0–11.8)	24.5 (6.3–50.6)	<0.0001
Apposition	n = 1,332	n = 1,632	
Frames with malapposed struts (n)	0.7 ± 1.9	2.4 ± 3.7	0.0006
Frames with malapposed struts (%)	0 (0–0)	0 (0–19.8)	0.0008
Maximum length of consecutive malapposed struts (mm)	0.6 ± 1.3	1.7 ± 2.7	0.001
Malapposition area (mm^2)	0.07 ± 0.22	0.25 ± 0.49	0.012
Maximum malapposition area (mm^2)	0.78 ± 2.66	1.20 ± 1.91	0.005
Maximum malapposition distance (mm)	0.20 ± 0.44	0.47 ± 0.81	0.02
Neoatherosclerosis	n = 1,332	n = 1,643	
Frames with neoatherosclerosis (n)	8.7 ± 5.9	0.0 ± 0.0	<0.0001
Frames with neoatherosclerosis (%)	43.4 (20.2–67.9)	0 (0–0)	<0.0001
Interstrut cavities	n = 1,349	n = 1,614	
Frames with interstrut cavities (n)	0.74 ± 2.7	1.2 ± 2.6	0.34
Frames with interstrut cavities (%)	0.0 (0–0)	0.0 (0–7.7)	0.06
Maximum interstrut cavities depth (mm)	0.11 ± 0.36	0.12 ± 0.19	0.90

Values are mean ± SD or median (interquartile range).

DISCUSSION

In the present study we investigated the frequency, timing, and etiologic factors of neoatherosclerosis in patients presenting with VLST to 29 European clinical centers with intravascular imaging capability. In this regard, the most salient findings of the present study can be summarized as follows: 1) neoatherosclerosis was observed in 58 of 134 patients (43.3%) with VLST; 2) in-stent plaque rupture was found to be the dominant underlying cause in 40 of 134 patients (30%) presenting with VLST at a median duration of 5.95 years from index stenting; 3) macrophage infiltration was abundant in frames showing in-stent plaque rupture, whereas calcification was more frequent in frames without plaque rupture; 4) implantation of DES was significantly associated with formation of neoatherosclerosis, whereas previous myocardial infarction in patients with neoatherosclerosis was strongly associated with plaque rupture; and 5) no significant difference was observed in histological thrombus composition between patients with and without neoatherosclerosis.

In-stent neoatherosclerosis was frequently observed in patients with VLST. In-stent plaque rupture was identified as the dominant pathological mechanism causing VLST in 30% of patients presenting beyond the 1-year time frame. Although the aim of the present analysis was to provide insights into the frequency and timing of neoatherosclerosis in a patient population presenting with VLST, in which the absolute frequency of neoatherosclerosis is expectedly high, the 30% relative frequency of in-stent plaque rupture is of concern considering the enormous number of stents implanted on a global scale. In a recent analysis of patients presenting with VLST and undergoing OCT evaluation, Taniwaki et al. (3) reported findings of striking similarity related to the frequency of neoatherosclerosis (27.6%) considered to be causative for the occurrence of VLST in 58 patients (20 next- and 38 first-generation DES). The most frequent underlying cause of VLST was reported to be malapposition in 34.5% of stents in this report, which is different from our analysis and likely explained by the nature of procedural flow, whereby we aimed to acquire intravascular imaging pull-backs without causing artificial distortion of vessel anatomy by performing angioplasty before OCT imaging. The latter procedure was performed in approximately 26% of cases in the study by Taniwaki et al. (3) and likely revealed a greater proportion of malapposed stent struts following dislodgment of thrombus fragments prior to imaging. In another recent OCT analysis of

FIGURE 3 Cox Proportional Hazards Regression Analyses for Neoatherosclerosis and Plaque Rupture

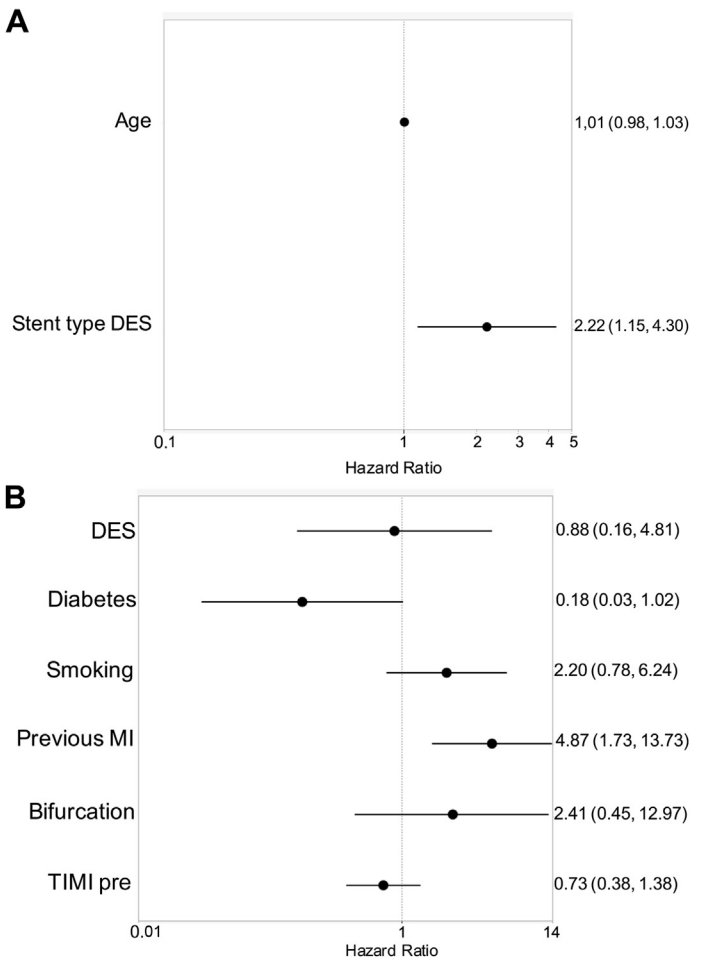

(A) Forest plot illustrating hazard ratios of covariates associated with neoatherosclerosis formation resulting from multivariate Cox proportional hazards regression analysis. **(B)** Forest plot illustrating hazard ratios of covariates in patients with neoatherosclerosis associated with plaque rupture resulting from multivariate Cox proportional hazards regression analysis. DES = drug-eluting stent(s); MI = myocardial infarction; TIMI = Thrombolysis In Myocardial Infarction.

patients presenting with VLST to 10 South Korean hospitals with OCT imaging capability, neoatherosclerosis was also found to be the most frequent cause of VLST (34.7%) in a total of 98 patients, followed by malapposition (33.7%) and uncovered stent struts (24.5%) (8). One of the key parallels among the 3 studies discussed is the fact that newer generation DES were consistently affected by neoatherosclerosis to a level that is similar to first-generation DES.

Given the significantly longer duration of implantation in BMS relative to DES, we performed multivariate Cox regression analysis to identify factors associated with the formation of neoatherosclerosis and plaque rupture. Strikingly, the implantation of DES was significantly associated with the formation of neoatherosclerosis. It has recently been reported that leaky endothelial cell junctions give rise to accelerated atheroma formation within the nascent neointima following DES implantation, resulting from prolonged release of antiproliferative drugs known to impede endothelial integrity during recovery after vascular injury (9). Therefore, neoatheroma formation may occur earlier after DES implantation compared with BMS implantation, which has been suggested in autopsy studies (1), recent intravascular imaging trials (10), and the present registry. Although duration from index stenting was strongly associated with neoatherosclerosis formation by univariate analysis, and BMS tended to cluster within the VLST group, only the implantation of DES turned out to be significantly associated with neoatherosclerosis by multivariate Cox regression analysis.

In a recent autopsy study, the earliest time point at which foam cell formation within the peristrut neointimal tissue was observed was 70 days following paclitaxel-eluting stent and 120 days following sirolimus-eluting stent implantation, which contrasts with the 900-day time span reported for BMS (1). Similarly, fibroatheroma with necrotic core formation within neointimal tissue was observed as early as 270 days following paclitaxel-eluting stent placement, 360 days following sirolimus-eluting stent placement, and 900 days following BMS placement, respectively. Most important, unstable neoatherosclerotic plaque features such as thin-cap fibroatheroma formation and plaque rupture were observed within 2 years following first-generation DES implantation and 5 years following BMS placement. In keeping with this trend, the earliest plaque rupture in DES occurred at 1.6 years following index stenting in the present set of data, whereas the shortest time span to plaque rupture in BMS was 2.5 years.

Importantly, pathology data from a large series of autopsy cases suggested that underlying vulnerable plaque type is associated the occurrence of neoatherosclerosis over time with both DES and BMS (9), which is supported by the increased risk for plaque rupture in patients with previous myocardial infarction in our study. Future prospective clinical studies are needed to confirm this intriguing hypothesis.

In the present analysis, stent area was significantly larger in patients with neoatherosclerosis, which may point toward increased susceptibility of neoatherosclerosis formation in coronary segments of

large diameter. In line with seminal pathology studies (11), which showed that formation of native atherosclerotic plaque is more frequently observed in proximal coronary segments, neoatherosclerosis may be very much akin to native atherosclerotic plaque with regard to preferential development in proximal stented vascular segments.

Foam cell infiltration of neointimal tissue has been proposed to be the earliest sign of neoatherosclerosis formation (9). Interestingly, signal attenuation indicative of macrophage infiltration was significantly more frequent in OCT frames with plaque rupture versus those without, suggesting that significant macrophage infiltration might be associated with plaque vulnerability in rupture-prone neoatherosclerotic lesions. Furthermore, calcification was more often observed in OCT frames without plaque rupture, confirming previous studies (12) suggesting calcification to be a marker of plaque quiescence. Whether calcification has a direct protective effect and whether its role contributed to the occurrence of VLST remains to be studied. Fibrous cap thickness measured 115 ± 15 μm in our study, which contrasts with the average cap thickness of 65 μm of vulnerable plaque prone to rupture in seminal autopsy studies (13). It is likely that imprecision of measurements attributable to limitations in the axial resolution of OCT imaging and tissue shrinkage during histopathologic processing explain these differences. Furthermore, a recent histopathologic validation study addressed potential differential diagnosis of OCT findings including neoatherosclerosis and found that significant light attenuation suggestive of macrophages and neoatherosclerosis may also be caused by other tissue components including elastic fibers (14). Consequently, additional histopathologic validation studies are required to confirm our findings.

An intriguing finding relates to the predictive power of prior myocardial infarction in patients with VLST caused by in-stent plaque rupture. Susceptibility to plaque rupture may be the common denominator in these patients and causative during the onset of myocardial infarction (plaque rupture of native arterial coronary segment) as well as during the onset of VLST (in-stent plaque rupture). One might hypothesize that patients who experienced plaque rupture as a cause of myocardial infarction and treated by primary percutaneous coronary intervention may be at increased risk for future plaque rupture within stented coronary segments.

No significant differences were observed in thrombus composition among patients with and those without neoatherosclerosis in the present analysis. In a previous analysis, we assessed composition in a total of 253 thrombus specimens from patients with stent thrombosis undergoing thrombus aspiration (4), which did not reveal significant differences in terms of thrombus composition as a function of time (early vs. late stent thrombosis). Overall, thrombus aspirates were heterogeneous in composition, containing platelet-rich thrombus, fibrin fragments, erythrocytes, and inflammatory cells. Leukocytes were present in most thrombus samples in significant numbers, with neutrophil subpopulations accounting for most cells, highlighting the important role of inflammatory cell recruitment in ST; importantly, thrombus composition of samples acquired in the setting of VLST does not significantly deviate from published data reporting findings from plaque rupture in native coronary arteries (15). Consequently, formation and composition of arterial thrombosis can be explained as acute response-to-injury cascade, which is likely determined by platelet reactivity, peripheral leukocyte counts, and individual patient-specific phenotype, rather than being influenced by the presence or absence of neoatherosclerosis. Irrespective of this acute response-to-injury cascade resulting in thrombus formation, stent-associated inflammatory reactions are likely to affect neoatherosclerosis formation, which has been suggested in human autopsy studies (16). Future studies are needed to more clearly decipher acute blood-borne immune reactions versus peristrut inflammatory reactions in the pathogenesis of neoatherosclerosis and its manifestation as VLST.

STUDY LIMITATIONS. Our study had important limitations, one of them being the absence of a control group of patients with similar duration of implantation in the absence of VLST. Although important parameters such as the relevance of asymptomatic neoatherosclerotic change within neointimal tissue in patients following stent implantation may have been derived from such a cohort, the design and structure of our registry were limited to patients presenting with stent thrombosis. Consequently, the findings of the present study are descriptive in nature and intended to be hypothesis generating, which warrants confirmation in randomized prospective trials. Furthermore, the selection of patients must be considered when interpreting the results of our present study. Because only percutaneous coronary intervention centers with OCT capability were included to collect cases for the present analysis, the

data may not be representative of a broader patient population. Also, the presence of significant residual thrombus likely affects the assessment of underlying pathologies. Last, manual thrombectomy and predilatation with small-sized balloons were performed in a considerable number of patients presenting with VLST, which may have influenced imaging assessment of plaque rupture and neoatherosclerosis.

CONCLUSIONS

We have shown that in-stent plaque rupture represents a frequent and often fatal consequence of neoatherosclerosis formation in patients with VLST. Implantation of DES was associated with increased risk for neoatherosclerosis formation over time, whereas plaque rupture often occurred in patients with neoatherosclerosis and previous myocardial infarction. Although sample size was limited for the present analysis, we achieved approximately 70% power to detect a 2-fold increased hazard ratio to develop neoatherosclerosis after DES implantation compared with BMS. Macrophage infiltration within neointimal tissue may be used as an imaging surrogate for plaque vulnerability in future trials investigating the clinical relevance of neoatherosclerosis formation following stent implantation.

ADDRESS FOR CORRESPONDENCE: Prof. Dr. Michael Joner, Deutsches Herzzentrum München, Klinik an der Technischen Universität München, Lazarettstrasse 36, 80636 Munich, Germany. E-mail: joner@dhm.mhn.de.

PERSPECTIVES

WHAT IS KNOWN? Neoatherosclerosis has recently been introduced as novel disease manifestation of atherosclerosis within the nascent neointima following stent implantation.

WHAT IS NEW? We collected the largest sample size of patients suffering from very late stent thrombosis undergoing OCT imaging. For the first time we provided clinical evidence and confirmation that DES are associated with earlier formation of neoatherosclerosis when compared to BMS.

WHAT IS NEXT? Future clinical studies with prospective imaging design will have to establish the clinical prevalence of neoatherosclerosis in patients in symptomatic and asymptomatic patients.

REFERENCES

1. Nakazawa G, Otsuka F, Nakano M, et al. The pathology of neoatherosclerosis in human coronary implants: bare-metal and drug-eluting stents. J Am Coll Cardiol 2011;57:1314–22.

2. Takano M, Yamamoto M, Inami S, et al. Appearance of lipid-laden intima and neovascularization after implantation of bare-metal stents extended late-phase observation by intracoronary optical coherence tomography. J Am Coll Cardiol 2009;55:26–32.

3. Taniwaki M, Radu MD, Zaugg S, et al. Mechanisms of very late drug-eluting stent thrombosis assessed by optical coherence tomography. Circulation 2016;133:650–60.

4. Riegger J, Byrne RA, Joner M, et al. Histopathological evaluation of thrombus in patients presenting with stent thrombosis. A multicenter European study: a report of the prevention of late stent thrombosis by an interdisciplinary global European effort consortium. Eur Heart J 2016;37:1538–49.

5. Cutlip DE, Windecker S, Mehran R, et al. Clinical end points in coronary stent trials: A case for standardized definitions. Circulation 2007;115:2344–51.

6. Wenaweser P, Rey C, Eberli FR, et al. Stent thrombosis following bare-metal stent implantation: Success of emergency percutaneous coronary intervention and predictors of adverse outcome. Eur Heart J 2005;26:1180–7.

7. Adriaenssens T, Joner M, Godschalk TC, et al. Optical coherence tomography findings in patients with coronary stent thrombosis: a report of the PRESTIGE Consortium (Prevention of Late Stent Thrombosis by an Interdisciplinary Global European Effort). Circulation 2017;136:1007–21.

8. Lee S, Ahn J, Mintz GS, et al. Characteristics of earlier versus delayed presentation of very late drug-eluting stent thrombosis: an optical coherence tomographic study. J Am Heart Assoc 2017;6:e005386.

9. Otsuka F, Byrne RA, Yahagi K, et al. Neoatherosclerosis: overview of histopathologic findings and implications for intravascular imaging assessment. Eur Heart J 2015;36:2147–59.

10. Kim C, Kim B-K, Lee S-Y, et al. Incidence, clinical presentation, and predictors of early neoatherosclerosis after drug-eluting stent implantation. Am Heart J 2015;170:591–7.

11. Virmani R, Burke AP, Kolodgie F. Morphological characteristics of coronary atherosclerosis in diabetes mellitus. Can J Cardiol 2006;22:81B–4B.

12. Virmani R, Joner M, Sakakura K. Recent highlights of ATVB: calcification. Arterioscler Thromb Vasc Biol 2014;34:1329–32.

13. Virmani R, Kolodgie FD, Burke AP, Farb A, Schwartz SM. Lessons from sudden coronary death: a comprehensive morphological classification scheme for atherosclerotic lesions. Arterioscler Thromb Vasc Biol 2000;20:1262–75.

14. Lutter C, Mori H, Yahagi K, et al. Histopathological differential diagnosis of optical coherence tomographic image interpretation after stenting. J Am Coll Cardiol Intv 2016;9:2511–23.

15. Cook S, Ladich E, Nakazawa G, et al. Correlation of intravascular ultrasound findings with histopathological analysis of thrombus aspirates in patients with very late drug-eluting stent thrombosis. Circulation 2009;120:391–9.

16. Otsuka F, Yahagi K, Ladich E, et al. Hypersensitivity reaction in the US Food and Drug Administration–approved second-generation drug-eluting stents. Circulation 2015;131:322–4.

KEY WORDS imaging, neoatherosclerosis, stent thrombosis

APPENDIX For supplemental tables and figures, please see the online version of this paper.